THE EFFECT OF GROWTH TIME ON THE PROPERTIES OF LPCVD GROWN WO_3 THIN LAYERS FOR ELECTROCHROMIC APPLICATIONS

LOULOUDAKIS D.[1], VERNARDOU D.[1,2], SUCHEA M.[1,2], DAVAZOGLOU D.[3], KOUDOUMAS E.[1,2]
[1] *Center of Materials Technology and Photonics, School of Engineering, Technological Educational Institute of Crete*
[2] *Department of Electrical Engineering, School of Engineering, Technological Educational Institute of Crete*
[3] *NCSR "Demokritos," Institute of Nanoscience and Nanotechnology*
koudoumas@staff.teicrete.gr

This work presents the effect of growth time on the structural, morphological and electrochemical properties of WO_3 thin layers grown by low pressure chemical vapor deposition (LPCVD). ϒ-monoclinic WO_3 crystalline phase and granular agglomerations structure with thickness from <20 nm up to 80 nm were successfully obtained onto FTO coated glass substrates using tungsten hexacarbonyl ($W(CO)_6$) as a precursor at a 450°C substrate temperature, for deposition times of 5, 10, 15 and 20 minutes. The layers were characterized by XRD, Raman spectroscopy, FE-SEM and cyclic voltammetry in an effort to understand how the structural and morphological characteristics affect the electrochemical/electrochromic properties.

In the recent years, electrochromic windows have attracted a lot of attention, because they can offer dynamic modulation in a broad spectral range, to meet personal preferences. Compared with photochromic and thermochromic windows, electrochromic windows require full device configuration and electric supply, which complicates their design. In addition, electrochromic devices must meet particular requirements for architectural window applications. First, all components, that is transparent conductors, electrolytes, and charge storage materials, must be highly transparent to visible light, and must also have appropriate refractive index to minimize reflections. Second, all the components must be electrochemically stable within the switching voltage range. Finally, practical applications require the use of solid-state electrolytes, such as polymer ion gels or ion-conducting ceramics, as liquid electrolytes can leak, catch fire,

or even deform or break the glass owing to gravity, especially for large windows. The most popular electrochromic devices are based on a thin-film battery-type configuration, in which a layer of electrochromic material (metal oxide or conjugated polymer) is coated on a TCO working electrode, and a charge storage layer is coated onto a TCO counter electrode. These two electrodes are joined by a layer serving as an ion-conducting electrolyte and separator. In a typical configuration, the device darkens when ions are inserted into the electrochromic layer, and it bleaches when the ions are extracted. The magnitude of the color change can be controlled directly by the amount of inserted charge. These devices exhibit open circuit memory and can maintain a colored state for an extended period of time.

Transition metal oxides are suitable for electrochromic devices as electrochromic layer because they show considerable variation in stoichiometry, and can be quite easily deposited in form of thin films which is appropriate for device manufacturing. Among them, tungsten oxide (WO_3) is of large interest and has been extensively investigated due to its appreciable electrochromic properties in the visible and infrared region. It exhibits large optical modulation, good durability, low power consumption, less stress for the viewer's eyes, and relatively low price [1]. Electrochromic WO_3 thin films have been prepared by a large number of techniques, such as thermal evaporation, electrodeposition, spray pyrolysis, chemical vapor deposition, electron beam evaporation, magnetron sputtering, sol-gel [2 - 13] etc. Among these techniques, CVD can easily be integrated to float-glass lines, has fast deposition rate and the layer's properties can be easily controlled through the growth temperature (in the range of 400–600°C), O_2 flow rate etc.

In this work, γ-monoclinic WO_3 layers has been deposited on fluorine doped tin dioxide (FTO) glass substrates using a low pressure-CVD (LPCVD) system at 450°C for various deposition times. The layers were characterized by XRD, Raman spectroscopy, FE-SEM and cyclic voltammetry in an effort to understand how the structural and morphological characteristics affect the electrochemical/electrochromic properties.

Experimental conditions

Thin WO_3 layers were grown onto FTO coated glass substrates by LPCVD, using tungsten hexacarbonyl ($W(CO)_6$) as a tungsten precursor at a 450°C substrate temperature, and N_2 (carrier gas) and O_2 (in the reactor) flows of 0.05 liters/min, for deposition time of 5, 10, 15 and 20 minutes. These growth times corresponds to thicknesses of <20 nm for 5 min, and about 30, 50 and 80 nm for the longer times.

Structural analysis was performed in a Siemens D5000 Diffractometer using operating conditions: CuKα (λ = 1.54056 Å), 2θ= 20.0-50.0°, step time 60 s/° and a Nicolet Almega XR micro-Raman system for a range of 100-1000 cm-1 and a laser line at 473 nm. The morphology of the samples was examined in a Jeol JSM-7000F field-emission scanning electron microscope (FE-SEM) at an operating voltage of 15 kV. All samples were over-coated with a thin of gold prior to FE-SEM analysis to avoid charging. Electrochemical measurements were performed using a three-electrode cell as reported previously [14-17]. The measurements were accomplished using a scan rate of 10 mV s-1 through the voltage range of -1000 mV to +1000 mV. The area of the working electrode (working electrode refers to the WO_3 layer grown on FTO) exposed to the electrolyte was 1 cm^2. The lithium ion intercalation/de-intercalation process with respect to time was also studied using chronoamperometry at -1000 mV and +1000 mV for a step of 200 s and a total time period of 2000 s.

Results and discussions

All as-grown WO_3 layers were transparent over the whole area of the substrate and adherent passing the Scotch tape test (removal of an X shaped piece of sticking tape [18]). Fig. 1 shows the X-ray diffraction (XRD) patterns of WO_3 layers grown for 5, 10, 15 and 20 minutes onto clean FTO coated glass substrates.

The film grown for 5 min is amorphous, the XRD pattern presenting reflections only due to the FTO glass substrate at 26.5°, 33.7° with respective Miller indices (110), (101) and the aluminum sample holder [19]. For 10 min growth time, characteristic peaks at 23.3°, and 24.6° of the ϒ-monoclinic WO_3 crystalline phase corresponding to (002), and (200) crystalline orientations are observed [20-22]. Longer deposition times lead also to an additional small contribution from the (020) crystalline orientation of the same ϒ-monoclinic crystalline phase, at 23.8°. The XRD patterns of all layers show the reflections due to the FTO glass substrate at 26.5°, 33.7° and 37.1° with respective Miller indices (110), (101) and (200) and the Al sample holder. The highest intensity of the (002) peak in the XRD spectrum suggests a preferential orientation perpendicular to the thin film plane, i.e. along the c-axis. At room temperature, ϒ- monoclinic WO_3 is the most common and stable phase. Monoclinic WO_3 consists of planar arrays of corner-sharing WO_6 octahedra, placed perpendicular to the [001] hexagonal axis and held together along the z axis by Van de Waal's forces. In this structural configuration, the site of the missing cation B (compared to a perovskite-like atomic configuration with the ideal ABO3 cubic crystal

structure) is empty and easily accessible through tunnels present between the octahedra, thus allowing for ionic transport and intercalation within the structure in case of an external force.

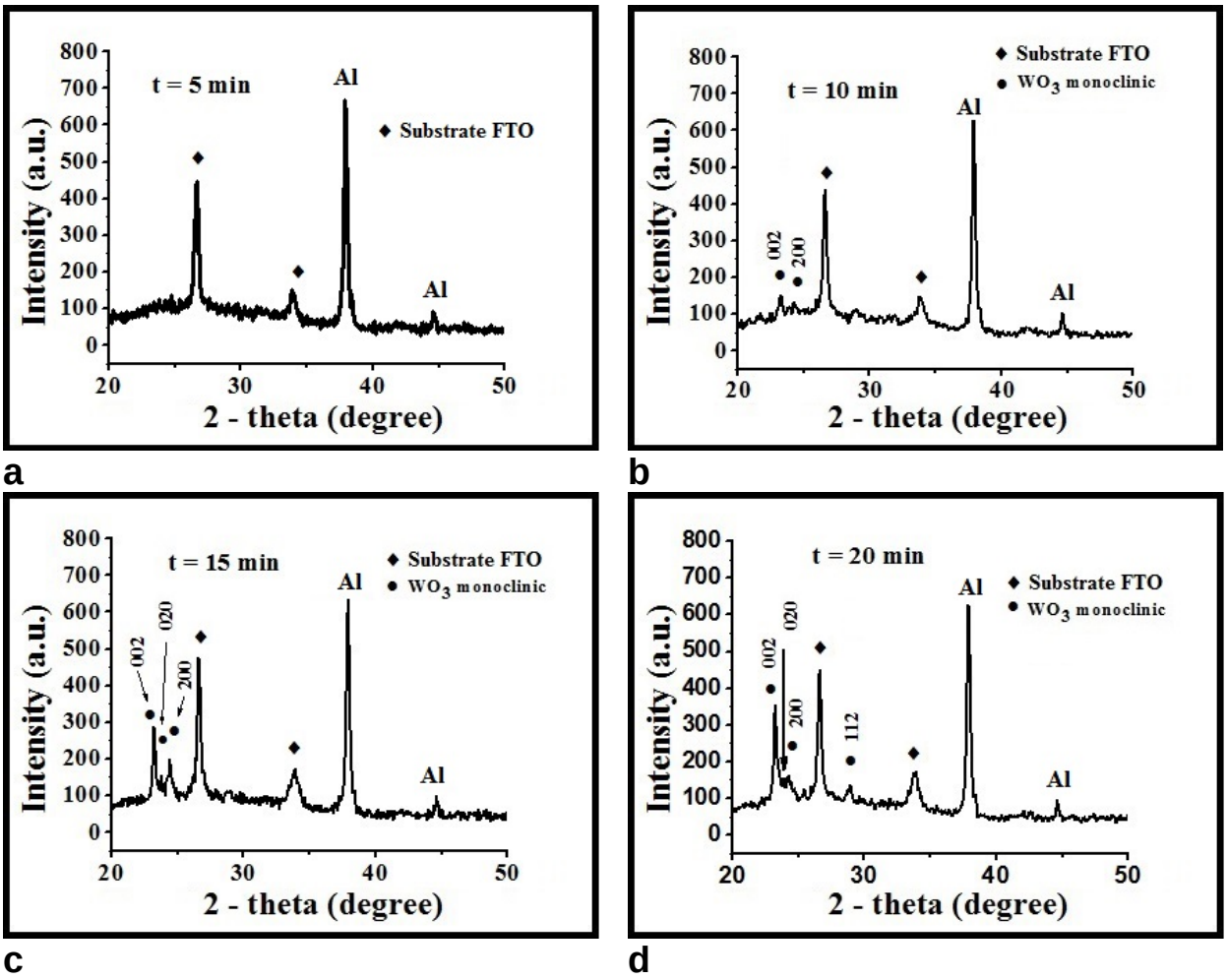

Fig. 1 X-ray diffraction (XRD) patterns of WO_3 layers grown by LPCVD for **a** 5, **b** 10, **c** 15 and **d** 20 minutes.

In its stable monoclinic phase, WO_3 exhibits high resistance against photocorrosion and strong chemical stability in acidic solutions, as reported by the Pourbaix diagram of tungsten [23]. The missing peaks of γ-monoclinic crystalline phase may be attributed to the fact that films have a thickness lower than 100nm and the strong substrate and holder contributions to the XRD pattern covers other weak reflections from the films.

Similarly, Raman spectroscopy confirmed the presence of monoclinic WO_3 phase for the films grown for longer times [24, 25]. Fig. 2 displays the Raman spectra of WO_3 for all samples. Raman peaks at the frequencies of

269 and 323 cm^{-1} are assigned the W-O-W bending modes of bridging oxide ions [24], while the W-O-W stretching mode (tungsten oxide network) correspond to the high frequency Raman peaks at 713 and 806 cm-1 [26].

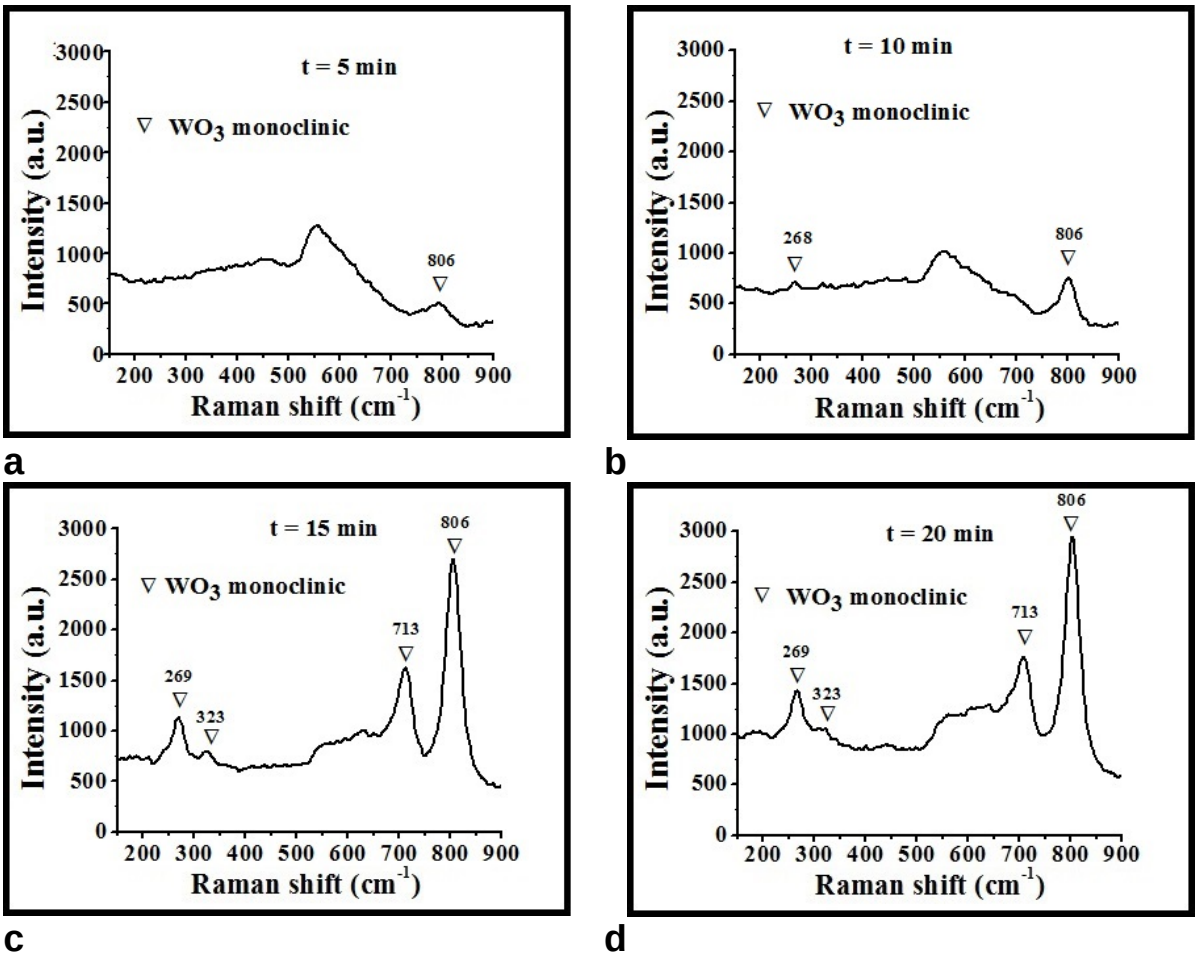

Fig. 2 *Raman spectroscopy of WO_3 layers grown by LPCVD for* ***a*** *5,* ***b*** *10,* ***c*** *15 and* ***d*** *20 minutes.*

The presence of the well-defined peaks in Raman spectroscopy compared with XRD reveals a trend towards crystallization that is however still small enough to lie below the detection limit of XRD [27].

FE-SEM analysis of the as-grown WO_3 films is shown in Fig. 3. In all cases, films showed a granular structure packed in agglomerations of grains. A decrease of grains size in agglomerations as the growth time increases and the film crystallinity is slightly improved can be observed in these images.

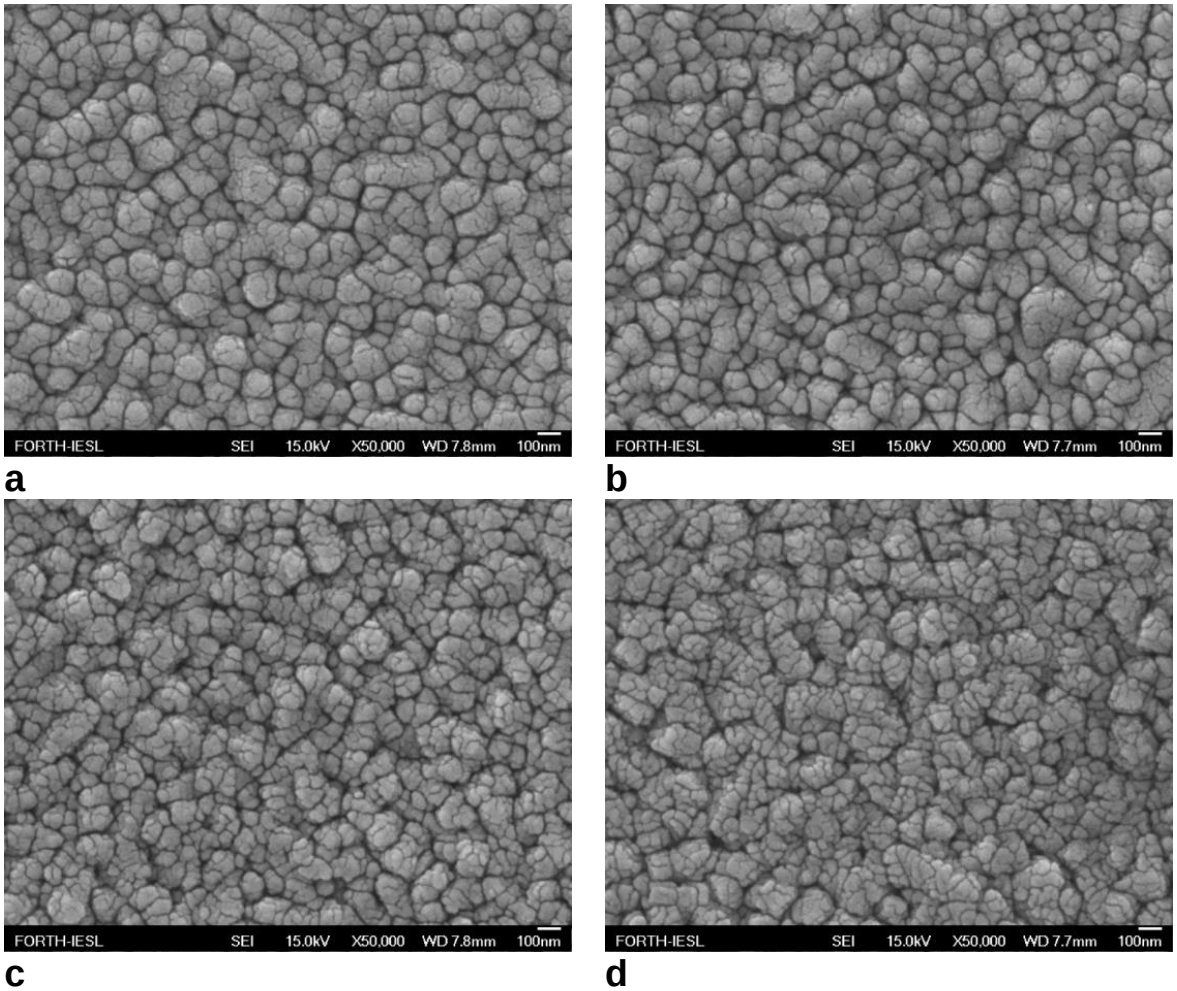

Fig. 3 FE-SEM imaging of WO_3 layers grown by LPCVD for **a** 5, **b** 10, **c** 15 and **d** 20 minutes.

In order to study the effect of the growth time, and the subsequent structural and morphological characteristics, on the electrochemical performance of the as-grown WO_3 layers, cyclic voltammogram curves were collected using a scan rate of 10 mV s^{-1} and 1 M $LiClO_4$/propylene carbonate as electrolyte and are presented in Fig. 4.

All of the curves are normalized to the geometric area of the working electrode, resulting in units of μA cm^{-2}. The as grown WO_3 layers were found to be transparent, while, after the intercalation of the Li+ ions, the color was changed to blue. The samples were becoming again transparent after the de-intercalation of the Li+ ions, of course when no ions were remaining within the WO_3 lattice.

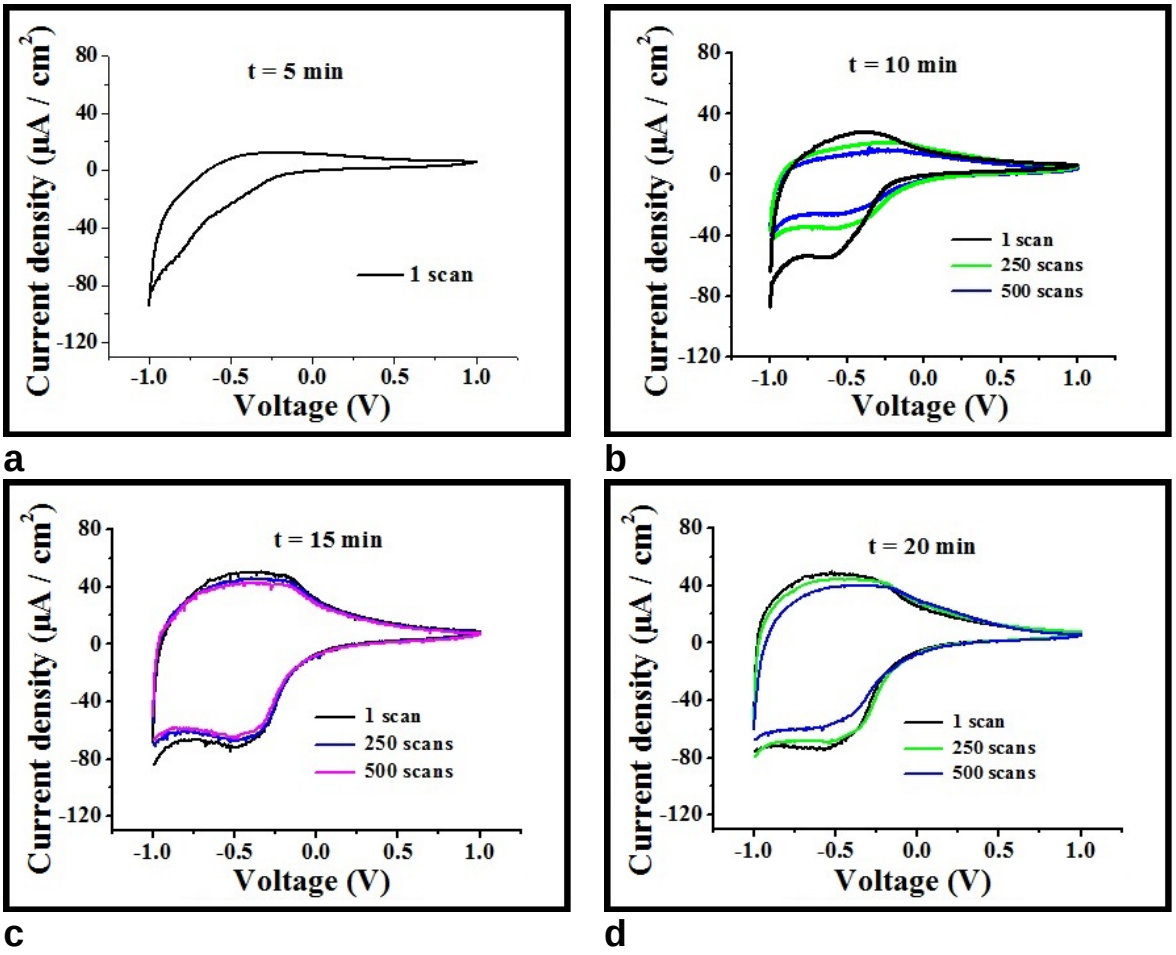

Fig. 4 Current-voltage curves of WO_3 layers grown by LPCVD for **a** 5, **b** 10, **c** 15 and **d** 20 minutes.

The coloring - discoloration process can be represented according to the equation

$$WO_3 \text{ (transparent)} + xLi^+ + xe^- \leftrightarrow Li_xWO_3 \text{ (blue)}$$

The results shown in Figure 4, can be summarized as following: in the sample grown for 5 min, no current was recorded after the first scan, possibly due to the dissolution of the respective layer (Fig 4a); the samples grown for 10 (Fig. 4b) and 20 min (Fig. 4d) present a more or less stable response for up to 250 cycles. After that, the sample presented degradation, indicated by a change in the shape of the curve and a shift of the maxima, a behavior that can be attributed to the non-reversibility of the process, leading in permanent presence of Li ions within the WO_3 lattice, which was evident by a remaining light blue color. The sample grown for 15 min appeared to have the best performance, presenting a very stable response even after 500 cycles. The maxima appeared at -0,5 V are attributed to the intercalation and the de-intercalation of the Li+ ions,

followed by the gain or the loss of an electron. Moreover, after the de-intercalation of the Li+ ions, the sample was becoming transparent (Fig 4c). Chronoamperometry tests were also conducted, switching the voltage between -1000 mV and +1000 mV at an interval of 200 s. The obtained curves for films grown for different time periods are shown in Fig. 5.

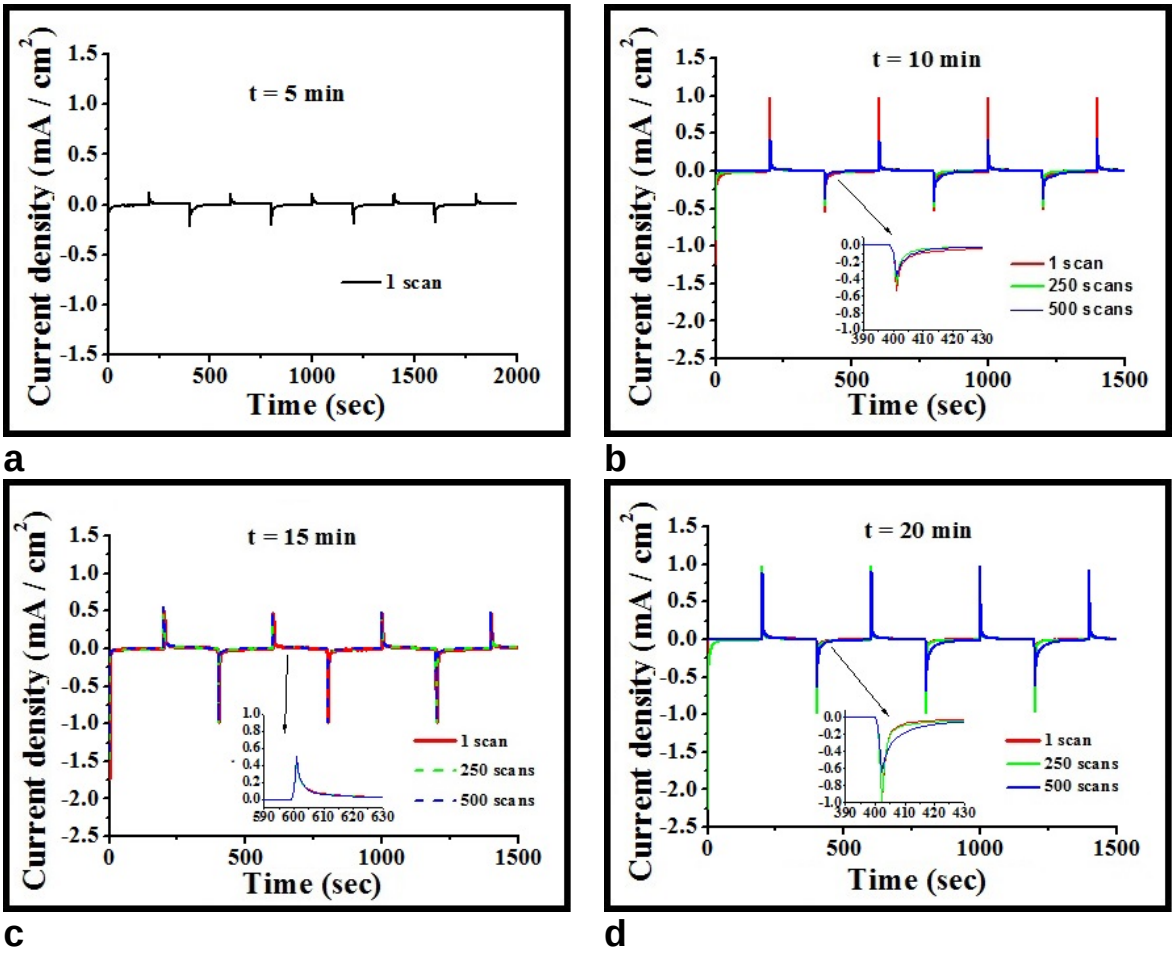

Fig. 5 Chronoamperometry measurements of WO_3 layers grown by LPCVD for **a** 5, **b** 10, **c** 15 and **d** 20 minutes.

In particular, the samples grown for 10 and 20 min were found to present a reduction of the current density with increasing cycle number after the 250th cycle, while in the 15 min sample, the current density was found constant up to the 500th cycle. The amount of Li+ charge interchanged between the layers and the electrolyte was calculated by integration of excess current densities measured are shown in table 1 together with the intercalation and de-intercalation times (from the 1st cycle results).

Table 1. Times and calculated Li+ charge interchanged between the layers and the electrolyte

Growth time (min)	Intercalation time (s)	De-intercalation time (s)	Intercalation charge (mC/cm^2)	De-intercalation charge (mC/cm^2)
10	19	14	4.03	1.63
15	13	7	4.11	3.80
20	14	9	4.30	2.68

As can be seen, the sample grown for 15 min presents the best performance, exhibiting faster response times and quite small number of ions remaining within the WO_3 lattice, the difference between intercalation and de-intercalation charge being around 7 % only. Besides that, this sample presented an only 16% reduction of the intercalation charge at the 250^{th} cycle.

Conclusions

In this work, the effect of growth time on the structural, morphological and electrochemical characteristics of WO_3 thin layers grown by low pressure chemical deposition (LPCVD) was investigated. It was found that layers of γ-monoclinic WO_3 crystalline phase and having granular agglomerations structure with thickness from <20 nm to 80 nm can be obtained at a 450°C substrate temperature, for deposition times of 10, 15 and 20 minutes. With increasing growth time, the crystallinity was improved and a decrease of the grains size in the agglomerations was induced. Optimum, fast and stable electrochemical response was found for a deposition time of 15 min, the respective layer exhibiting a difference between intercalation and de-intercalation charge of 7 % and presenting an only 16% reduction of the intercalation charge at the 250^{th} cycle.

References

[1] E. S. Lee, D. L. Di Bartolomeo,*Solar Energy Materials & Solar Cells*, 71(4) 465 (2002).

[2] C. G. Granqvist, Solar Energy Materials & Solar Cells, 60 201 (2000).

[3] M. C. Rao, O. M. Hussain, *Research Journal of Chemical Sciences*1 (7) 92 (2011).

[4] P. M. S. Monk, *Critical Reviews in Solid State and Materials Sciences* 24 193 (1999).

[5] A. J. More, R. S. Patil, D. S. Dalavi, S. S. Mali, M. G. Gang, J. H. Kim, *Materials Letters* 134 298 (2014).
[6] C. Y. Kim, S. G. Cho, S. Park, D. K. Choi, *Journal of Ceramic Processing Research* 10 (6) 851(2009).
[7] A. A. Joraid, *Current Applied Physic*s 9 73 (2009).
[8] R. U. Kirss, L. Meda, *Applied Organometric Chemistry* 12 155 (1998).
[9] D. Gogova, K. Gesheva, A. Szekeres, M. Sendova-Vassileva, *physica status solidi (a)* 176 969 (1999).
[10] C. M. Wang, C. Y. Wen, Y. C. Chen, K. S. Kao, D. L. Cheng, C. H. Peng, *Integrated Ferroelectrics: An International Journal* 158 (1) 62 (2014).
[11] T. S. Yang, Z. R. Lin, M. S. Wong, *Applied Surface Science* 252 (2) 2029 (2005).
[12] F. Zhang, H. Q. Wang, S. Wang, J. Y. Wang, Z. C. Zhong, Y. Jin, *Chinese Physics B* 23 (9) 098105(1-6) (2014).
[13] A. P. Baker, S. N. B. Hodgson, M. J. Edilisinghe*, Surface and Coatings Technology* 153 (2) 184 (2002).
[14] D. Vernardou, D. Louloudakis, E. Spanakis, N. Katsarakis, and E. Koudoumas, New J. Chem. 38, 1959 (2014).
[15] D. Vernardou, M. Apostolopoulou, D. Louloudakis, N. Katsarakis, and E. Koudoumas, New J. Chem. 38, 2098 (2014).
[16] D. Vernardou, M. Apostolopoulou, D. Louloudakis, N. Katsarakis, and E. Koudoumas, J. Colloid Interf. Sci. 424, 1 (2014).
[17] D. Vernardou, M. Apostolopoulou, D. Louloudakis, E. Spanakis, N. Katsarakis, E. Koudoumas, J. McGrath, and M.E. Pemble, J. Alloys Compd. 586, 621 (2014).
[18] T. D. Manning, I. P. Parkin, R. J. H. Clark, D. Sheel, M. E. Pemble, and D. Vernardou, J. Mater. Chem. 12, 2936 (2002).
[19] E. Elangovan and K. Ramamurthi, Thin Solid Films 476, 231 (2005).
[20] X. Hu, Q. Ji, J. P. Hill, and K. Ariga, Cryst. Eng. Commun. 13, 2237 (2011).
[21] H. Zhang, M. Yao, L. Bai, W. Xiang, H. Jin, J. Lin, and F. Yuan, Cryst. Eng. Commun. 15, 1432 (2013).
[22] Z. Lu, S. M. Kanana, and C. P. Tripp, J. Mater. Chem. 12, 983 (2002).
[23] M. I. Nave and K. G. Kornev, Metallurgical and Materials Transactions A, 48A, 1414 (2017).
[24] B. Pecquenard, H. Lecacheaux, L. Livage, and C. Julien, J. Solid State Chem. 135, 159 (1998).
[25] M. Boulova and G. Lucazeau, J. Solid State Chem. 167, 425 (2002).
[26] H. Habazaki, Y. Hayashi, and H. Konno, Electrochim. Acta 47, 4181 (2002).
[27] D. Vernardou, E. Spanakis, G. Kenanakis, E. Koudoumas, and N. Katsarakis, Mater. Chem. Phys. 124, 319 (2010).